needle-like materials and the effect on the diffraction pattern is the observation of enhanced intensity along specific crystallographic directions with a subsequent decrease of intensity along other directions.

A number of sample-presentation methods can be used to minimize preferred orientation. For flat specimens, back pressing and side drifting into the sample holder can be effective. These methods tend to produce much less preferred orientation than front-mounted samples, but tend not to be very effective for chronic preferred orientation such as that exhibited by phases like clays, feldspars and chlorite. Reducing the size of the crystallites improves the probability of achieving random alignment of the crystallites in the sample holder. Gradually milling a sample and monitoring the preferred-orientation coefficients as a function of grinding time may again help to find the correct, or at least reproducible, grinding conditions (Fig. 3.9.18).

A major advantage of whole-pattern-based QPA over single-peak methods is that all classes of reflections are considered in the calculation. In this sense, the method is less prone to preferred orientation of a particular class of peaks. Furthermore, orientation effects may be corrected by applying March–Dollase (Dollase, 1986) or spherical-harmonics (Ahtee *et al.*, 1989) corrections. A properly applied correction may be of high importance for QPA in cases where a phase is present at low concentration and only a few peaks can clearly be identified in the pattern. If those peak(s) are affected by preferred orientation, the March–Dollase coefficient correlates strongly with scale factors and leads to biased QPA results. Examples of this effect occur with layered materials that have sheet-like morphology perpendicular to the *c* axis, including mica and clay minerals, which typically show stronger than expected intensity for the 00*l* reflections.

The crucial factor seems to be to what extent the orientation parameters correlate with the Rietveld scale factor. An example where the correlation is only minor is sample 2 from the IUCr CPD round robin on QPA (Scarlett *et al.*, 2002). In that example, brucite [$Mg(OH)_2$] shows strong preferred orientation along the 00*l* direction. This may be corrected by the March–Dollase model, which returns a refined value of 0.66. However, the introduction of this preferred-orientation correction only changes the brucite concentration from 35 to 36 wt% (weighed = 36.36 wt%); this is surprising because the orientation is strong and the weighted residual R_{wp} changes from 30 to 15%. Close examination of the correlations reveals a strong correlation between the brucite scale factor and preferred-orientation factor.

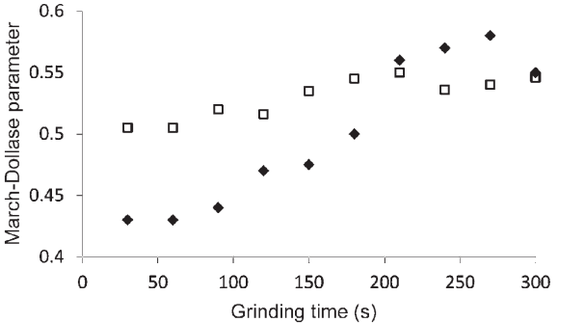

Figure 3.9.18
Increase of the March–Dollase (Dollase, 1986) parameter and related decrease of the degree of preferred orientation with grinding time for the two amphibole species actinolite (filled diamonds) and grunerite (open squares) in an iron ore. Data courtesy ThyssenKrupp – Resource Technologies (Knorr & Bornefeld, 2013).

However, the correlation of the brucite preferred-orientation parameter to the other scale factors (zincite, corundum and fluorite) is close to zero; this explains why in this example the QPA is not highly dependent on preferred orientation. In cases of strong correlation between the orientation parameter of one phase and the scale factors of other phases, preferred orientation should probably not be refined, or at least it should be verified carefully. It is worth noting that, in all Rietveld-based analyses, users should examine the correlation matrix as a matter of general practice to establish which parameters might be affecting parameters of interest.

It should be noted that sample rotation around the scattering vector (typically employed in flat-plate Bragg–Brentano geometry) during the scan does not reduce preferred orientation, since there is no change between the preferred-orientation direction and the diffraction vector. Using capillaries in transmission geometry assists in the reduction of preferred orientation, but the time-consuming nature of packing capillaries makes this technique infeasible in industrial applications where diffraction-based QPA is used for routine quality control.

3.9.10.3.3. *Microabsorption*

The strongest on-going impediment to accuracy in QPA using XRD data is microabsorption. The microabsorption effect occurs when a multiphase sample contains both low- and highly absorbing phases. For the highly absorbing phases, the X-ray beam is more likely to be absorbed in the surface layers of the grain; thus, the fraction of the grain contributing to the diffraction pattern will decrease as the size of the grain increases above the beam-penetration depth. For the low-absorbing phases, the beam penetrates further into the particle resulting in a greater likelihood of the desired 'volume diffraction' occurring (Brindley, 1945). The overall effect is the observation of a disproportionate amount of observed intensity from individual grains relative to what would be expected for the average absorption of the sample; the highly absorbing phases are under-represented relative to the low-absorbing phases. There is extensive discussion of the microabsorption issue in Zevin & Kimmel (1995).

Brindley (1945) has described the particle absorption contrast factor τ_α as

$$\tau_\alpha = (1/V)\int_0^V \exp\left(-(\mu_\alpha - \bar{\mu})\right) \mathrm{d}v, \qquad (3.9.48)$$

where V is the particle volume, and μ_α and $\bar{\mu}$ are the linear absorption coefficients of phase α and the entire sample, respectively. While it is relatively easy to calculate the absorption coefficients, equation (3.9.48) implies knowledge of the *particle* size of each component; this information is only available through independent microscope or light-scattering characterization.

This correction term is commonly incorporated into QPA through a modification to equation (3.9.26) of the form

$$W_\alpha = \frac{S_\alpha (ZMV)_\alpha / \tau_\alpha}{\sum_{k=1}^{n} S_k (ZMV)_k / \tau_k}. \qquad (3.9.49)$$

Brindley has also devised criteria by which to assess whether a microabsorption problem is likely to be present or not. Calculation of μD (where μ is the linear absorption coefficient and D is the particle diameter) yields the following criteria:

(i) $\mu D < 0.01$ – fine powder. There is negligible microabsorption and hence no correction is necessary.

Table 3.9.5
Calculated values of μD (where μ is the linear absorption coefficient and D is the particle diameter) for Cu $K\alpha$ X-rays for corundum, magnetite and zircon with a range of particle sizes

	μD		
Diameter (μm)	Corundum, Al_2O_3 (μ = 125 cm^{-1})	Magnetite, Fe_3O_4 (μ = 1167 cm^{-1})	Zircon, $ZrSiO_4$ (μ = 380 cm^{-1})
0.1	0.001	0.012	0.004
0.2	0.003	0.023	0.008
0.5	0.006	0.058	0.019
1	0.013	0.117	0.038
2	0.025	0.233	0.076
5	0.063	0.584	0.190
10	0.125	1.167	0.380
20	0.251	2.334	0.759

(ii) $0.01 < \mu D < 0.1$ – medium powder. Microabsorption is likely to be present and the normal Brindley correction model can be applied.

(iii) $0.1 < \mu D < 1.0$ – coarse powder. A large microabsorption effect is present. The Brindley model can only be used to provide an approximate correction provided that μD is closer to the lower limit of the range.

(iv) $\mu D > 1.0$ – very coarse powder. This indicates that severe microabsorption is likely to be present and that any correction is well beyond the limits of the model.

It is difficult for the analyst encountering a new sample to determine whether a correction for microabsorption is required without first obtaining additional information. A minimum requirement should be to calculate μD for each phase present. However, this requires knowledge of the particle size which, in a multiphase sample, can be very difficult to obtain unambiguously. Even when the particle size is measured by, for example, dynamic light scattering or optical or SEM image analysis, the applicability of the correction can still be unclear. In addition, the correction factor embodied in equations (3.9.48) and (3.9.49) makes the assumption that the particles of the phase of interest are spherical and of uniform size. This assumption is unrealistic in almost all samples; in reality, each phase is likely to be present at a wide range of particle sizes and the particles are highly unlikely to be spherical.

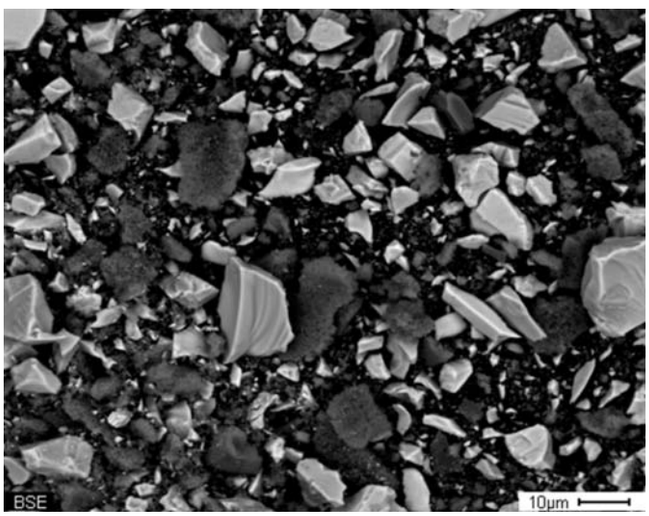

Figure 3.9.19
Backscattered-electron SEM image of a mixture of approximately equal amounts of corundum (dark grey), magnetite and zircon (lighter grey). Note the wide range of particle sizes present for each of the three phases.

Table 3.9.5 shows the calculated values of μD for Cu $K\alpha$ radiation for some commonly encountered phases in mineralogical analysis. For the least absorbing phase (corundum), the upper range of applicability of the Brindley model (medium powder) is reached at about 5 μm; by 8 μm, the coarse powder criterion has been reached and the correction model is no longer applicable. For magnetite, these limits are reached an order of magnitude earlier at about 0.5 and 0.9 μm, respectively.

Fig. 3.9.19 shows an SEM image of a mixture of approximately equal amounts of corundum, magnetite and zircon. The individual components of the sample were weighed and the mixture ground in ethanol in a McCrone micronizing mill (McCrone Research Associates, London) for 10 min g^{-1}. This approach to sample preparation is generally accepted as best practice for powder XRD because it minimizes structural damage during grinding (Hill & Madsen, 2002). After decanting and drying, the sample was back-packed into a cavity sample holder for XRD data collection; the same sample was then used to obtain the SEM image in Fig. 3.9.19. Visual observation shows a wide range of particle sizes (from submicron to greater than 10 μm) and shapes that do not even approximate spheres. Even if this information is obtained, selection of a particle size that best represents each individual phase is a difficult task. In addition, in many sample suites, the component phases exhibit a range of hardness resulting in different rates of grinding and hence difference size ranges. Regrettably, what happens too often in practice is that analysts will micronize the sample and then select an arbitrary particle size in order to derive a 'preferred' value for the final analysis. Therefore, caution is advised in the application of these correction models. The IUCr CPD round robin on QPA (Madsen *et al.*, 2001; Scarlett *et al.*, 2002) showed that many participants severely degraded their results by applying a correction when none was necessary.

Equation (3.9.48) shows that there two ways to minimize microabsorption. The first is to reduce the absorption contrast by, for example, changing the X-ray wavelength. While corundum and magnetite have very different linear absorption coefficients for Cu $K\alpha$ radiation (126 and 1123 cm^{-1}, respectively), the difference is reduced to 196 and 231 cm^{-1}, respectively, for Co $K\alpha$ radiation. The second approach is to reduce the particle size in order to meet Brindley's fine- or medium-powder criteria.

However, even these steps may not be sufficient to eliminate the microabsorption effect. Slightly different absorption coefficients, or different particle sizes for phases with the same absorption coefficients, may still introduce a bias between expected and analysed concentrations. In this situation, it may be better to use a calibrated hkl_phase or peaks_phase (Section 3.9.6) instead of a Rietveld, structure-based phase. The calibration step involved in the generation of such a phase incorporates the microabsorption problem into the calibration constant.

Fig. 3.9.20 shows the bias between known concentrations (derived from chemical analysis) and QPA-determined concentrations for a series of salt samples. The samples contain halite (NaCl), sylvite (KCl) and kieserite ($MgSO_4{\cdot}H_2O$) as major phases and small amounts of anhydrite ($CaSO_4$), langbeinite [$K_2Mg_2(SO_4)_3$] and carnallite [$KMgCl_3{\cdot}6(H_2O)$]. The linear absorption coefficient of sylvite (254 cm^{-1}) is much higher than halite (165 cm^{-1}). Using crystal-structure-based analysis, there is a systematic deviation of up to 3% with an overestimation of the low absorber (halite) and an underestimation of the high absorber (sylvite). After replacing sylvite by a calibrated

hkl_phase, the bias is reduced to about 1% and does not show systematic deviations.

It should be noted, however, that the phase constants developed using such a calibration approach will only be applicable to the sample suite and preparation conditions for which it was developed. The calibration process will need to be repeated if there are significant changes to the sample suite or sample-preparation conditions.

3.9.10.3.4. *Whole-pattern-refinement effects*

One of the distinct advantages of structure-based whole-pattern fitting for QPA is that no standards need to be prepared because the structure for each phase provides the phase constant *ZMV*; the unit-cell dimensions allow the calculation of the cell volume *V* and the unit-cell contents provide the mass *ZM* (Bish & Howard, 1988; Hill & Howard, 1987). These values are used, along with the Rietveld scale factor *S*, in equation (3.9.26) to derive the phase abundance. This is especially useful for complex systems where the preparation of multiple standards would add considerably to the analytical complexity.

An additional advantage is the ability to refine the crystal structure (unit-cell dimensions and site-occupation factors, for example), when the data are of sufficiently high quality, in order to obtain the best fit between observed and calculated patterns. In addition to updating the *ZMV* value, the site occupancies are contained in the structure-factor calculation and, therefore, will change the relative reflection intensities and have an impact on the scale factor and QPA. Other structural parameters that have a strong effect on the scale factor and QPA are the atomic displacement parameters (ADPs). Strong correlation between the ADPs and amorphous material concentration has been shown by Gualtieri (2000) and Madsen *et al.* (2011).

This leads to the question: which crystal structure should be selected for QPA? Databases contain multiple entries for the same phase with the structures determined using different methods. While ADPs and site-occupation factors determined using neutron diffraction and single-crystal analysis should be favoured over those determined using X-ray powder data, many database entries do not have refined ADPs for all (and in some cases, any) atoms. Often, arbitrarily chosen default values of 0.5 or 1.0 $Å^2$ for B_{eq} are entered for all atoms, but this should be viewed or used with great caution. There is clearly a need to carefully evaluate the crystal-structure data used for QPA. This is particularly worth mentioning in view of the advent of new 'user-friendly' software that automatically assigns crystal structures after having performed the phase identification.

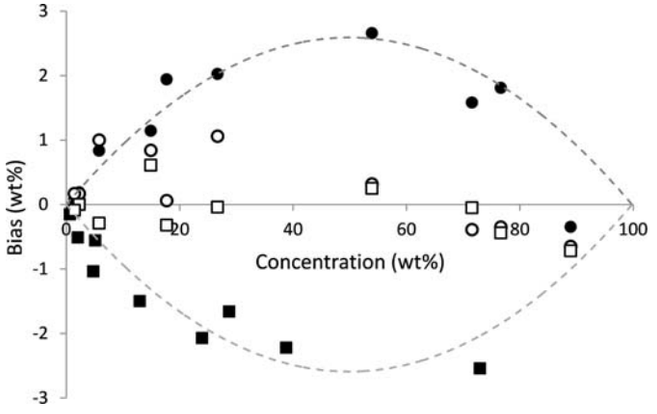

Figure 3.9.20
Bias as a function of phase concentration for industrial salt samples for (i) structure-based QPA (filled symbols) and (ii) calibrated hkl_phase (open symbols) for halite (circles) and sylvite (squares). The broken lines indicate the trend of the bias for structure-based QPA. Data are courtesy of K+S AG, Germany.

Empirical profile-shape models contribute significantly to the complexity (and correlations) of whole-powder-pattern fitting for QPA because of the large number of phases and multiple parameters required to model the profile shape of each phase. The use of convolution-based profile fitting [in, for example, *BGMN* (Bergmann *et al.*, 1998, 2000) and *TOPAS* (Bruker AXS, 2013)] greatly reduces the number of parameters, because the instrument-resolution function (which is constant for a given setup) can be separated from sample-related peak broadening. The instrument component can be refined using a standard and then fixed for subsequent analysis. The sample contribution to peak width and shape can then be related directly to crystallite size and microstrain using a minimal number of parameters. The reduction of the total number of parameters reduces the refinement complexity and the chance of parameter correlation.

The choice of the function used to model the pattern background may also have a strong influence on amorphous content (Gualtieri, 2000; Madsen *et al.*, 2011). Given that the intensities of both the background and the amorphous contribution vary slowly as a function of 2θ, it is inevitable that there will be a high degree of correlation between them. Hence, any errors in determining the true background will result in errors in amorphous phase determination. A simple approach is to use a background function with a minimal number of parameters. A more exact approach requires the separation of the amorphous contribution from background components such as Compton scattering and parasitic scattering by the sample environment and air in the beam path. This is routinely done in pair distribution function (PDF) analysis; details can be found in Chapter 5.7 in this volume and in Egami & Billinge (2003).

Another parameter that correlates with the pattern background is the width of broad peaks for phases of low concentration. If allowed to refine to very large width values, the peaks are 'smeared' over a broad range of the pattern with no clear distinction between peaks and background. The same issue applies when there is a high degree of peak overlap, particularly at high angles, leading to severe under- or over-estimation of the phase. The careful use of limits for either crystallite size or corresponding parameters in empirical peak-shape modelling assists in minimizing this effect.

There can be a subtle interplay between the profile-shape function and the pattern background that has an impact on whole-pattern fitting (Hill, 1992). The data in Fig. 3.9.21, collected using a Cu tube and an Ni $K\beta$ filter, exhibit low-angle truncation of the peak tails at the β-filter absorption edge. On the high-angle side, the anatase peak displays a wide tail which extends to the position of the strongest rutile peak at about 27.5° 2θ. In this case, rutile is present as a minor phase and the error in the background determination using conventional peak-profile modelling (Fig. 3.9.21*a*) introduces about 0.5% bias in the rutile QPA. The use of a more accurate profile model that incorporates the effect of the β-filter absorption edge (Fig. 3.9.21*b*) serves to improve the accuracy (Bruker AXS, 2013).

3.9.10.3.5. *Element analytical standards*

XRD-based derivation of elemental abundances relies on (i) the QPA abundances, and (ii) the assumed or measured stoichiometry of the crystalline phases. The accuracy of the QPA